

Objective Climatology of Cyclones in the Mediterranean Region

ISABEL F. TRIGO AND TREVOR D. DAVIES

Climatic Research Unit, University of East Anglia, Norwich, United Kingdom

GRANT R. BIGG

School of Environmental Sciences, University of East Anglia, Norwich, United Kingdom

(Manuscript received 10 February 1998, in final form 19 June 1998)

ABSTRACT

An objective cyclone detection and tracking analysis is performed over an 18-yr period, for the Mediterranean basin. The high-resolution ($1.125^\circ \times 1.125^\circ$ grid) European Centre for Medium-Range Weather Forecasts data used in this study proved to be particularly suitable for the detection and tracking techniques and to identify subsynoptic-scale Mediterranean lows, which have often been underestimated in previous studies.

The major characteristics of Mediterranean cyclones are examined and compared with other Northern Hemisphere depressions. Both cyclogenesis and cyclolysis regions are identified in the domain of study. In addition, characteristics of Mediterranean depressions, such as cyclone duration and intensity, as well as their persistence throughout the year, are shown to be quite variable for different formation areas. Overall, the regions where cyclogenesis is mainly controlled by topography, like the Gulf of Genoa and south of the Atlas Mountains, seem to generally account for the most intense events.

Finally, a statistical analysis based on a k -means clustering procedure summarizes trajectory information obtained from the 18-yr climatology. The method proved to be efficient in grouping cyclone paths from similar cyclogenesis regions and with similar characteristics of movement, showing generally more clusters in the western Mediterranean than in the eastern part of the basin.

1. Introduction

The climate of the Mediterranean region is conditioned by its position in the transition area between the subtropical high pressure belt and the midlatitude westerlies. Many of its characteristics and variability are, therefore, associated with upper air circulation (e.g., Jacobeit 1987). However, its unique weather features are also highly influenced by the almost enclosed Mediterranean Sea itself, representing an important source of energy and moisture for cyclone development, and by its complex land topography, which plays a major role in steering air flow.

In the context of cyclogenesis and in particular, the role of the sea, the Mediterranean basin may be described as a "climate test basin" (Garrett et al. 1993). Many of the cyclones experienced in the region either originate over the sea itself or are reinforced by it. The Mediterranean may then be considered a closed system, where both the sea's influence on cyclone characteristics

and variability and their feedback over the sea are worth investigating. An objective and detailed climatology of cyclone development and behavior for the area would be of relevance for a more complete understanding of the dynamics of the atmosphere in the subtropical margins, and the relationship between cyclones and air-sea fluxes variables, as well as for possible projections of future storm climatologies and their implications for local weather conditions.

In previous climatological analyses of Northern Hemisphere cyclones (e.g., Petterssen 1956; Lefevre and Nielsen-Gammon 1995), it is possible to detect some of the main Mediterranean centers of activity, such as the two winter cyclone maxima separated by the Italian peninsula, and the summer Iberian and North African maxima. However, the dependence of local weather, particularly strong winds and/or precipitation conditions, on cyclone preferential paths demands a more detailed description of the cyclogenesis areas and of cyclone movement.

Studies focused on the Mediterranean area, such as HMSO (1962), Radinovic (1987), and Flocas (1988) presented cyclone climatologies based on the analysis of pressure charts while, more recently, Alpert et al. (1990a) introduced objective methods to detect and track Mediterranean cyclones for a 5-yr climatology.

Corresponding author address: Dr. Isabel F. Trigo, Climatic Research Unit, University of East Anglia, Norwich NR4 7TJ, United Kingdom.
E-mail: i.trigo@uea.ac.uk

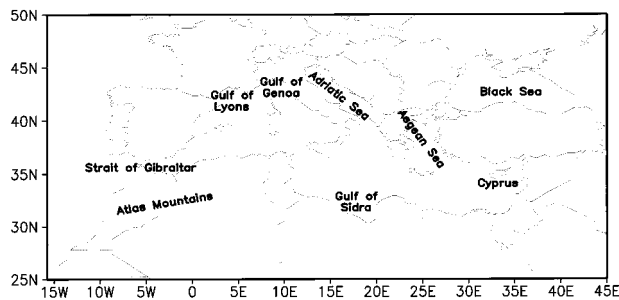


FIG. 1. Domain of study, limited between 24.75° and 50.625°N and between 15.75°W and 45°E. Most of the geographical names referred to in the text are also indicated in the figure.

The 18-yr European Centre for Medium-Range Weather Forecasts (ECMWF) dataset employed in the present paper allows a different approach, in particular (a) the cyclone detection and tracking schemes (described in section 2) are greatly simplified due to the high temporal and spatial resolution of the dataset; (b) subsynoptic-scale systems, usually underdetected in the previous works, are fully included; and (c) the objective climatology of Mediterranean cyclones may be considered more representative due to the relatively long dataset. Additionally, Mediterranean cyclone characteristics are examined region by region and compared with the results obtained for similar studies of other Northern Hemisphere weather systems (section 3).

To complete the picture of Mediterranean cyclone behavior, a climatology of storm tracks is also examined in terms of prevailing paths, velocities, and source regions. In contrast to previous works (e.g., Flocas 1988; Alpert et al. 1990b), a greater number of trajectories, including those for subsynoptic lows, is analyzed. The results are then summarized by submitting the monthly trajectories to a *k*-means clustering procedure (section 4).

2. Data and methodology

The data used in this study consist of ECMWF initialized reanalyses, available for the period between 1979 and 1996. Details about ECMWF model formulation, physics, and data assimilation may be found in ECMWF (1995).

The high temporal resolution (6-h) and spatial resolution (T106 horizontal spectral representation, which was interpolated to a $1.125^\circ \times 1.125^\circ$ regular grid), enabled us to use relatively simple algorithms both to detect and track cyclones, employing only the geopotential height field at 1000 hPa (Z_{1000}). There was no need to introduce any further interpolation schemes to optimize the finding of low pressure centers, such as those suggested by Alpert et al. (1990a) or by Murray and Simmonds (1991).

The data cover the area from 24.75° to 50.625°N and 15.75°W to 45°E, encompassing all the Mediterranean Sea and the surrounding regions (shown in Fig. 1): here-

after this area will be referred to as the “Mediterranean region.”

The algorithm implemented to detect cyclones in the Mediterranean region follows quite closely that described by Blender et al. (1997). A cyclone candidate is identified as a local Z_{1000} minimum, over a 3×3 gridpoint area. To be considered a cyclone, this minimum must fulfill two conditions: 1) a maximum value of 1020 hPa is required for the central sea level pressure evaluated as $p_{cen} \text{ (hPa)} = 0.121Z_{1000} \text{ (gpm)} + 1000$ (Peixoto and Oort 1992); and 2) the mean pressure gradient, estimated for an area of $9^\circ \text{ lat} \times 11.25^\circ \text{ long}$ around the minimum pressure, must be at least $0.55 \text{ hPa (100 km)}^{-1}$. These thresholds were found empirically, in order to eliminate small and weak troughs that were probably spurious artefacts of the high-resolution dataset.

Sinclair (1994) pointed out that important biases, such as a poleward displacement of the central low’s position and a tendency to favor the detection of the deeper or slower-moving systems, may occur, particularly under strong westerly flow, by employing sea level pressure (or Z_{1000}) algorithms instead of the pressure Laplacian (or geostrophic vorticity). However, we shall neglect both effects: not only is the surface eastward flow in the Mediterranean weaker than in Sinclair’s region of study (Southern Hemisphere midlatitudes), but the $1.125^\circ \times 1.125^\circ$ resolution should tend to overcome the second, and most important, bias effect.

For each cyclone detected, the distance between the central position and the nearest saddle point in the Z_{1000} field, that is, the distance between the center and the outermost closed isobar, is taken as a measure of the cyclone radius (Nielsen and Dole 1992).

The cyclone tracking algorithm is based on a nearest-neighbor search procedure, as described by Blender et al. (1997) and by Serreze et al. (1997): a cyclone’s trajectory is determined by computing the distance to cyclones detected in the previous chart and assuming the cyclone has taken the path of minimum distance; if the nearest neighbor in the previous chart is not within an area determined by imposing a maximum cyclone velocity of 33 km h^{-1} in the westward direction and of 90 km h^{-1} in any other, then cyclogenesis is assumed to have occurred. Again, these thresholds were determined empirically for this specific region by observing Mediterranean cyclone behavior in Z_{1000} charts.

A subjective analysis carried out for three months (January, April, and August 1979) revealed a success rate of over 96% for both detecting and tracking algorithms, suggesting good performances, independent of the time of the year.

3. Mediterranean cyclones

a. General characteristics

Over 60% of all the detected lows last for less than 12 h (Fig. 2). Most of these short-lived centers corre-

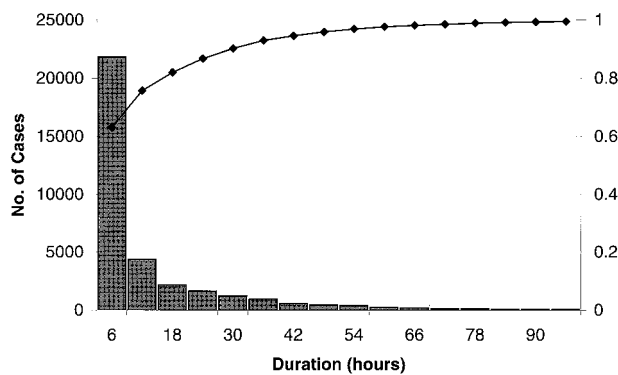


FIG. 2. Histogram of the detected cyclones' lifetimes.

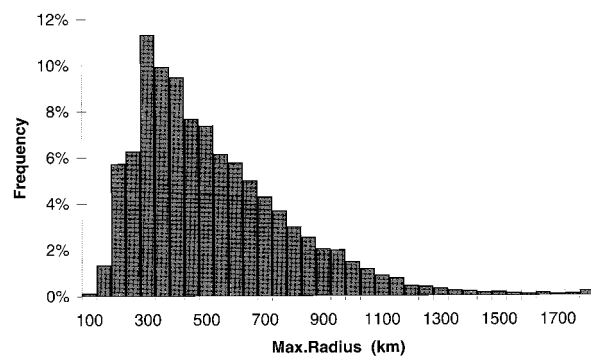


FIG. 3. Maximum radius distribution, obtained for all set of detected cyclones with a minimum life cycle of 12 h.

spond either to weak troughs with little activity or to secondary minima within complex systems, not deep enough to last more than a few hours or to develop into an individual low. Moreover, the shortest-lived of these detected minima might still be a result of the high-resolution dataset. These situations are therefore partially filtered by considering only cyclones that last a minimum of 12 h in all the subsequent analysis. This leaves about 55 cyclones per month. Taking this constraint into account, cyclones in the Mediterranean region have an average lifetime of 28 h, far less than the typical values of 3–3.5 days for North Atlantic or for North American synoptic systems (Blender et al. 1997; Nielsen and Dole 1992).

The maximum radius, obtained for each cyclone as described above, is regarded as a mere indicator of the spatial scale associated with Mediterranean lows. Its highly skewed distribution, estimated using the whole 18-yr period (Fig. 3) has an average of less than 500 km. Over 65% of the cyclones have a maximum radius less than 550 km, suggesting that most of the Mediterranean lows are within the mesoscale or subsynoptic-scale range, in contrast to synoptic North Atlantic systems, which have an expected maximum radius of 1000–2000 km (Nielsen and Dole 1992). A correlation of 0.39, statistically significant at the 95% level, was obtained between lifetime and maximum radius, indicating, as expected, that larger-scale systems are generally the most persistent. Moreover, this association might be underestimated, since large-scale systems also tend to leave the relatively small domain of this study rather than die within it.

As will be discussed in the next section, there are three distinct seasons in the Mediterranean region, with respect to cyclogenesis: winter, spring, and summer. We consider January, April, and August results as representative of these three seasons. Autumn's traditional months (September, October, and November) more easily fall either into the (late) summer or (early) winter categories.

Figure 4 shows the distributions of maximum deepening for January, April, and August. It should be noted

that positive values are obtained when the first cyclone detection also corresponds to the position of minimum central pressure during its life cycle. Following several authors (e.g., Roebber 1984), the deepening rate has been adjusted geostrophically to a reference latitude, φ_{ref} , in order to take into account the fact that cyclones at different latitudes with similar gradients would produce different geostrophic winds, and so should not be considered to have identical intensities:

$$dp/dt_{\text{adj}} = (dp/dt)(\sin\varphi_{\text{ref}}/\sin\varphi),$$

where dp/dt represents the deepening rate and φ the latitude. The midlatitude of the domain of study, approximately 37.5°N, was chosen for φ_{ref} .

Although the most frequent deepening rates do not change significantly throughout the year, being typically -2 or -1 hPa $(6 \text{ h})^{-1}$, winter and spring distributions show a greater skewness, as less pronounced deepening events occur during the summer. Similarly shaped distributions were obtained by Serreze (1995) for North Atlantic and Arctic winter cyclones, though they generally exhibit deeper cyclogenesis, with rates about 2–3 hPa $(6 \text{ h})^{-1}$ greater than in the Mediterranean (taking into consideration the latitude effect).

It is worth investigating the interdependence of cyclone features. Figures 5 and 6 show scatterplots of the minimum central pressure, estimated during each cyclone's lifetime, versus its maximum gradient over an $9^\circ\text{lat} \times 11.25^\circ$ long area and versus its maximum radius, respectively. The correlation coefficients between minimum pressure and maximum gradient range from -0.56 in March to -0.67 in August, being -0.63 on average. As expected, maximum radius also tends to increase with decreasing minimum central pressure. The relationship between this two variables is slightly less stable through the year, with correlations between -0.40 in August and -0.62 in December (annual mean ~ -0.52). The more widely scattered points around the regression lines occur for the most intense events, as may be found in all diagrams in Figs. 5 and 6. Artificial thresholds are visible in both figures for maximum gradient [the minimum value admitted is 0.55 hPa $(100$

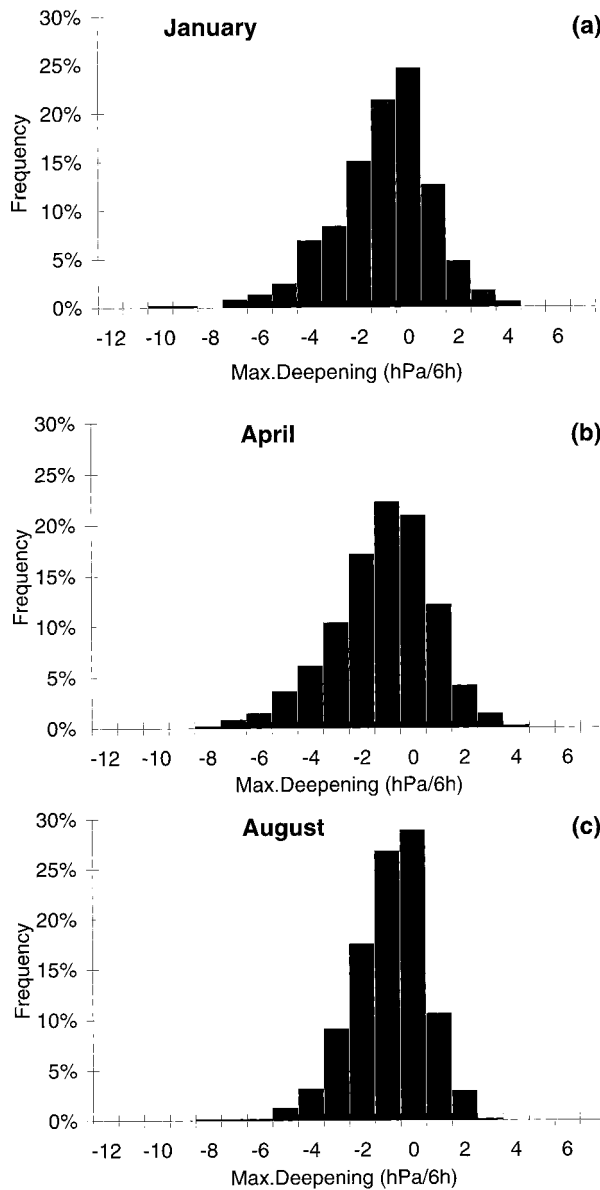


FIG. 4. Maximum deepening rate distributions, adjusted geostrophically to 37.5°N , for (a) Jan, (b) Apr, and (c) Aug. Negative values indicate deepening.

km^{-1})] and radius (minimum values obtained are of the order of 120 km) due to the conditions imposed in the search algorithm and to the spatial resolution of the dataset.

b. Sources and sinks

Overall, the monthly frequency distributions of cyclogenesis events, represented in Fig. 7 where the number of first cyclone detections per $2.25^{\circ} \times 2.25^{\circ}$ cell is plotted, indicate the existence of three main seasons: a winter season between October and March, spring between March and June, and summer between June and

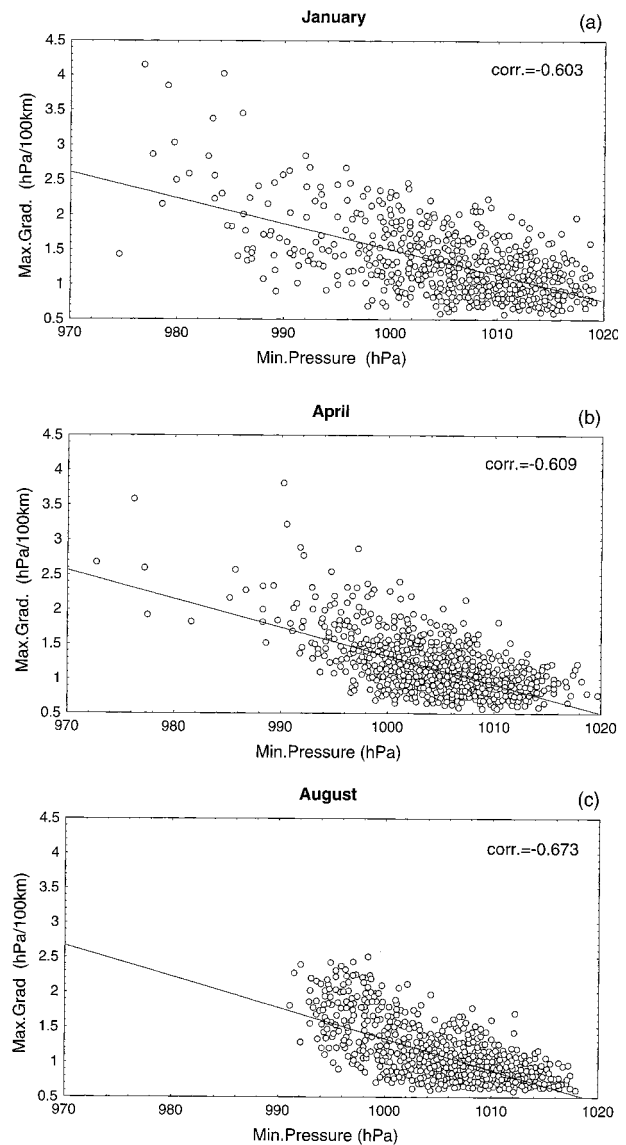


FIG. 5. Frequency scatterplots of maximum pressure gradient vs minimum central pressure, for (a) Jan, (b) Apr, and (c) Aug.

October. In particular, it is worth noting that October constitutes a rather sudden transition between the summer spatial pattern, still observed in September (Fig. 7i) and the winter pattern, already settled in November (Fig. 7k).

Figure 7 suggests that there are a number of areas, apparently primarily determined by the topography of the region, where cyclogenesis events tend to be concentrated. The western Mediterranean basin seems to be dominated by three main cyclogenesis regions.

1) The Genoa center, where cyclones are formed mostly in the lee of the Alps (Buzzi and Tibaldi 1978), constitutes one of the major cyclogenesis regions of the entire domain of study and one of the most persistent through the year. Figure 7 clearly shows the

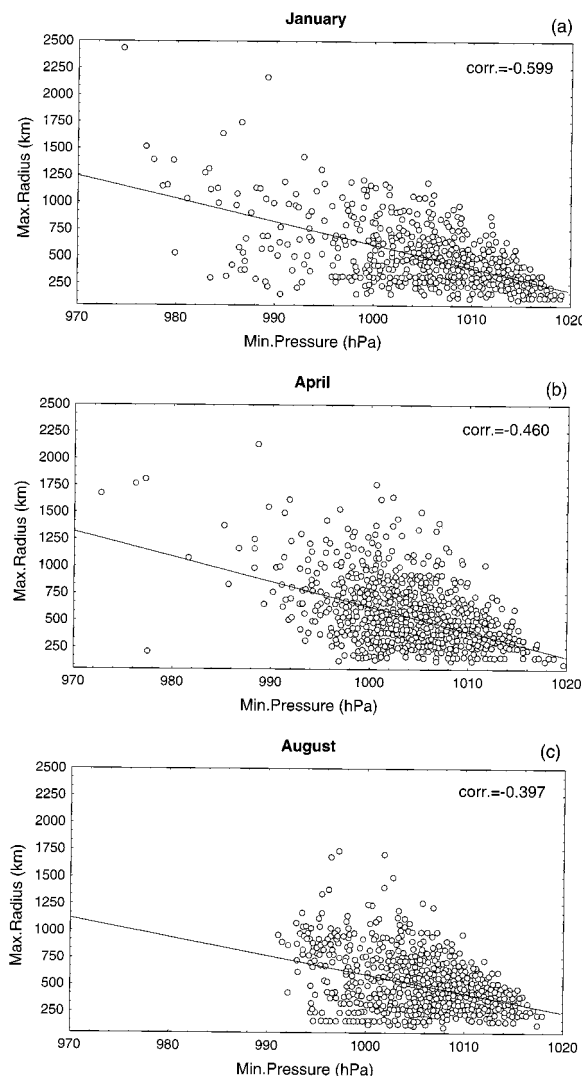


FIG. 6. As in Fig. 5, but for maximum radius vs minimum central pressure.

spreading of the Gulf of Genoa maximum into the Gulf of Lyons and the Balearic Islands, on the one hand, where weaker individual centers may be seen, and to distinct local maxima over the southern part of Italy (this is designated a separate region in Table 1 in order to establish whether or not its cyclones have different characteristics from those formed over the Gulf of Genoa).

- 2) Saharan cyclones (or Sharav depressions) seem to be the dominant feature of the Mediterranean spring, as the area south of the Atlas Mountains becomes a major source of cyclones. The western North African maximum is the most pronounced of the three, visible throughout the whole year and reaching its peak in May–June. Lee cyclogenesis is thought to play an important role in these Saharan lows (Egger et al. 1995), along with a dust influence amplifying radiative heating profiles (Thorncroft and Flocas 1997),

though the maximum observed over the North African Atlantic coast seems to be induced mainly by the sea–land contrast during the warmest season.

- 3) The relatively warm land, and sea–land contrast, also favors the formation of thermal lows over the Iberian peninsula from late spring through the summer. A three-core structure—over eastern and western coasts and central Iberia—becomes particularly pronounced between June and August.

The cyclogenesis in the eastern part of the domain seems to be distributed among four main regions.

- 1) The Aegean Sea is one of the major winter and spring cyclone sources. Due to its subsynoptic scale, Aegean cyclogenesis (Flocas and Karacostas 1996) has been frequently underestimated in previous Mediterranean cyclones studies (e.g., Alpert et al. 1990a).
- 2) A major cyclogenesis maximum occurs over the eastern Black Sea throughout the whole year, becoming particularly pronounced in July and August, when an average of one cyclogenesis event per week should be expected.
- 3) Cyprus.
- 4) The Middle East, observed over Syria and Iraq.

Both of these latter two cyclone maxima constitute the major summer characteristic of the eastern Mediterranean, mainly as a result of semipermanent extension of the Indian monsoon low. The Middle East cyclogenesis maxima is probably overestimated due to being near the domain's boundary. However, it shows high cyclone frequency, particularly between July and September. Despite the high cyclone activity observed near the surface, the upper troposphere over the eastern Mediterranean is dominated by strong descent as part of the Asian monsoon (Rodwell and Hoskins 1996), explaining the dry summertime climates of the region. More discussion on the mechanisms for creating the cyclones will be addressed in future work.

Based on the previous description, we will now focus on the properties of cyclones formed within each of the eight Mediterranean cyclogenesis regions, defined in Table 1. The monthly relative contribution of each region to all Mediterranean cyclogenesis events is presented in Fig. 8. It is worth noting that these relatively highly active regions account roughly for only 40%–50% of all detected events. There is a small, but significant, background of cyclone events spread widely over the region, constituting the remaining ~50% of events. Also the geographical range of each region explains, for instance, why Iberian peninsula cyclogenesis appears in Fig. 8 to be greater than zero during the whole year, despite the apparent lack of activity in winter (Figs. 7a,b,c,k,l).

The overall averages of cyclone duration (Table 2) and maximum radius (Table 3) are fairly constant throughout the year. However, both maximum gradient and deepening rate averages for the whole Mediterra-

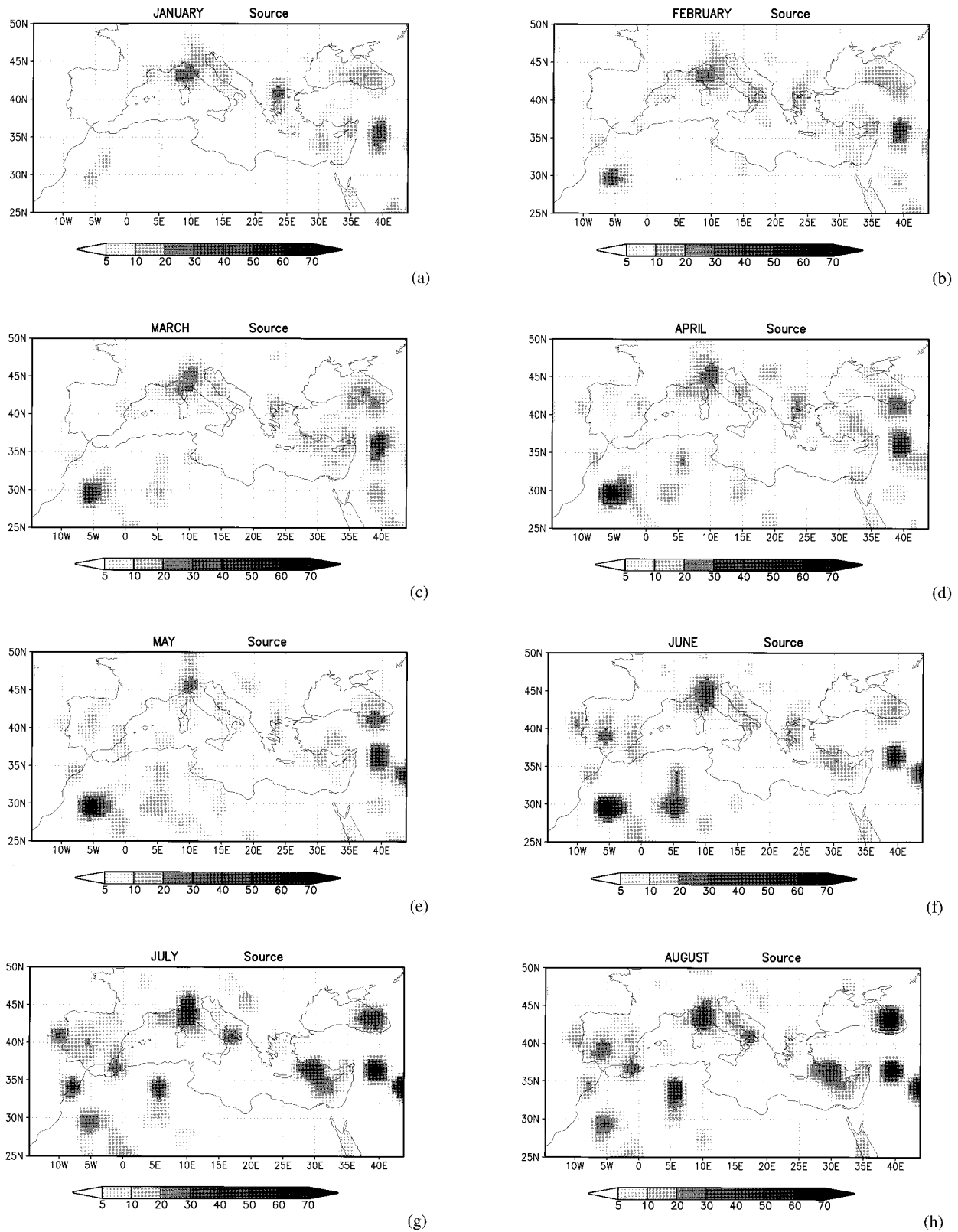


FIG. 7. Number of cyclogenesis events detected per $2.25^\circ \times 2.25^\circ$ cell, for each month, for the whole 18-yr period.

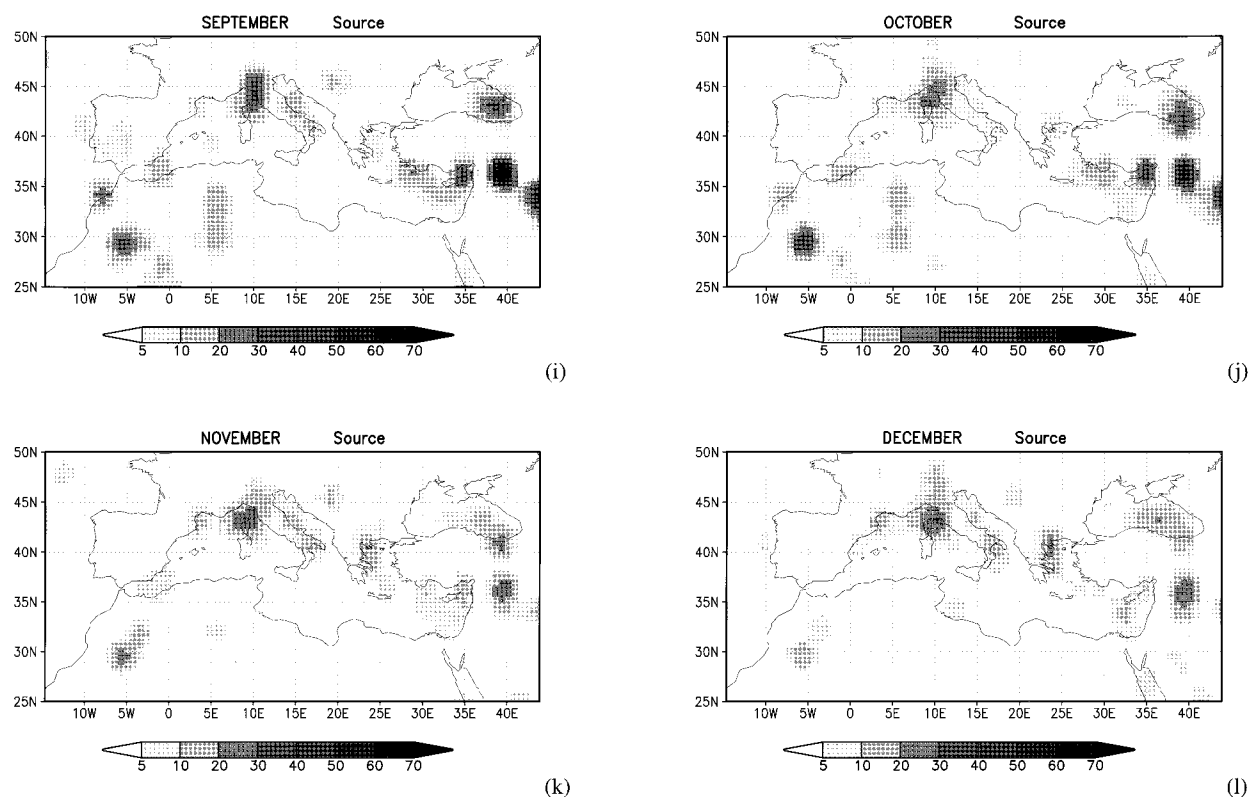


FIG. 7. (Continued)

mean decrease considerably toward the summer (Tables 4 and 5).

Although the cyclone frequency maximum in the Gulf of Genoa is present in all months (Fig. 7), the winter radius (Table 3) and intensity, measured by maximum gradient and deepening rate (Tables 4 and 5), are lower during spring and summer. Their life cycles, however (about 31 h, Table 2), are above average for the whole year. Also, it should be pointed out that, considering the relatively high latitude of the Gulf of Genoa, the winter cyclone's average radius is quite large by Mediterranean standards. The Aegean and Black Sea centers are also characterized by decreasing intensity toward the summer, despite the Black Sea's increasing cyclone frequency.

The Saharan region shows signs of very strong cy-

clogenesis events during spring. Moreover, the mean maximum deepening rate obtained for April Saharan lows appears to be considerably higher than that estimated for winter's most cyclogenetic region, the Gulf of Genoa. Lee cyclogenesis seems to be the main mechanism associated with both regions. However, the yet unexplored thermal effects of warm land and particularly of dust may be responsible for the high intensity of Sharav depressions, overcoming the lack of moisture and of latent heat release.

Cyprus and Middle East cyclones have higher inten-

TABLE 1. Cyclogenetic regions in the Mediterranean basin.

Name	Domain	Season
Sahara	28°–32°N; 7.5°–2.5°W	Spring and summer
Gulf of Genoa	40°–45°N; 7.5°–12.5°E	whole year
Southern Italy	38°–42°N; 15°–19°E	Winter
Cyprus	34°–38°N; 32.5°–37.5°E	Spring and summer
Middle East	32°–38°N; 37.5°–42.5°E	Spring and summer
Aegean Sea	36°–40°N; 22.5°–27.5°E	Winter and spring
Black Sea	41°–45°N; 32.5°–42.5°E	whole year
Iberian peninsula	36°–42°N; 10°W–0°	Summer

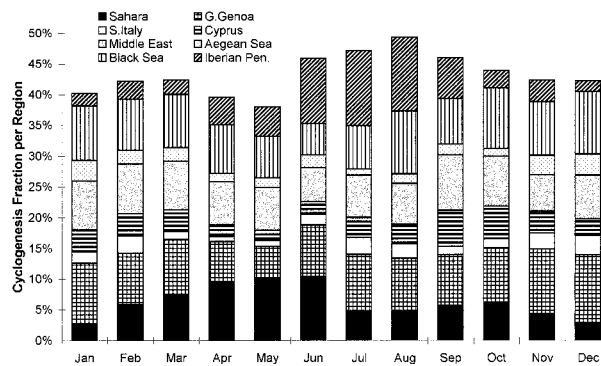


FIG. 8. Monthly fraction of cyclogenesis events occurred within each region.

TABLE 2. Average and standard deviation of cyclone duration (h) per cyclogenetic region.

	January		April		August	
	Mean	Std dev	Mean	Std dev	Mean	Std dev
Sahara	—	—	34.6	25.5	26.2	15.3
Gulf of Genoa	30.5	21.6	30.9	19.4	32.0	23.6
Southern Italy	28.0	17.8	23.5	7.3	—	—
Cyprus	22.7	18.9	23.5	13.5	25.1	21.7
Middle East	28.7	16.0	24.1	14.8	52.9	42.7
Aegean Sea	24.9	14.2	28.9	15.4	—	—
Black Sea	29.0	18.8	23.1	12.9	22.5	21.0
Iberian peninsula	—	—	—	—	24.0	18.2
Whole area	27.9	18.9	26.6	19.6	28.8	25.5

sities and lifetimes toward the summer. In the Middle East, August is characterized by very frequent and persistent cyclones, lasting for more than 52 h on average, which supports the link to monsoon mechanisms.

The difference between the number of first and last cyclone detections per $2.25^\circ \times 2.25^\circ$ cell is plotted in Fig. 9 for January, April, and August. It is possible to identify in all diagrams regions characterized by dipoles of cyclogenesis and cyclolysis, indicating the preferential directions of cyclone movement (section 4). It is interesting to note that, over the southern part of Italy, a cyclolysis maximum overcomes the cyclogenesis center depicted in Fig. 7, suggesting a southeastward movement of Gulf of Genoa cyclones. The most pronounced absolute maxima in Fig. 9 seem to occur in April and August over regions of relatively slow moving cyclones such as North Africa, with west-to-east movement in spring and summer and a second north-to-south dipole in August; Cyprus, with a strong northwest-to-southeast dipole during the summer; and the Black Sea east-to-west dipole, due to mainly stationary summer lows.

Traveling cyclones, however, are not well depicted in this kind of analysis. In order to examine the preferential paths of Mediterranean cyclones in more detail, a statistical analysis of cyclone tracks is presented in the next section.

4. Cyclone tracks

To summarize the 18-yr climatology of Mediterranean cyclone tracks we use cluster analysis based on a

k-means procedure. The *k*-means algorithm (e.g., Mirkin 1996) starts by defining *k* random clusters. In further steps, elements are rearranged between the groups in order to minimize variability within clusters and maximize variability between them. This particular method is quite different from other clustering analyses, for which no a priori hypotheses are needed. Since the goal of the *k*-means algorithm is to produce exactly *k* different clusters of greatest possible distinction, a preanalysis of the data is required to determine possible values for *k*.

In this study, the cluster analysis is performed over vectors containing the 6-h positions of each cyclone. Since all vectors undergoing the analysis must have the same dimension, only cyclones lasting a minimum of 36 h are taken into account. Also, the remaining positions of more persistent cyclones are not considered. This constraint means that only 10% of the detected cyclones are considered. However, between 200 and 370 tracks per month are still available for analysis. Before performing the *k*-means algorithm, monthly tracks are classified into two sets, corresponding to cyclones formed in the western Mediterranean (first longitude $<22.5^\circ\text{E}$) and in the eastern Mediterranean (first longitude $>22.5^\circ\text{E}$). This separation is suggested by Fig. 7 and has the advantage of allowing the search of fewer clusters per analysis, making the interpretation of results easier. To make sure that longitude and latitude have the same weight during the clustering process, all the coordinates within each set are standardized. Finally, the monthly sets of trajectory vectors are submitted to

TABLE 3. Average and standard deviation of maximum radius (km) per cyclogenetic region.

	January		April		August	
	Mean	Std dev	Mean	Std dev	Mean	Std dev
Sahara	—	—	589	284	531	263
Gulf of Genoa	526	344	481	202	385	153
Southern Italy	521	279	518	315	—	—
Cyprus	331	128	458	261	453	203
Middle East	323	134	375	221	454	334
Aegean Sea	501	230	498	191	—	—
Black Sea	381	168	387	140	398	140
Iberian peninsula	—	—	—	—	411	119
Whole area	473	281	520	276	481	240

TABLE 4. Average and standard deviation of maximum gradient [$\text{hPa (100 km}^{-1})$] per cyclogenetic region. All values have been adjusted to 37.5°N reference latitude.

	January		April		August	
	Mean	Std dev	Mean	Std dev	Mean	Std dev
Sahara	—	—	1.44	0.357	1.24	0.264
Gulf of Genoa	1.23	0.456	1.12	0.359	0.93	0.292
Southern Italy	1.29	0.535	1.20	0.382	—	—
Cyprus	1.02	0.339	1.02	0.236	1.10	0.423
Middle East	1.24	0.381	1.15	0.325	1.86	0.362
Aegean Sea	1.38	0.678	0.99	0.244	—	—
Black Sea	1.25	0.367	1.08	0.291	0.88	0.220
Iberian peninsula	—	—	—	—	0.89	0.190
Whole area	1.24	0.452	1.16	0.380	1.07	0.391

several experiments using values of k suggested by a subjective analysis of the data, ranging from 6 to 9 for the western Mediterranean and from 4 to 8 in the eastern Mediterranean.

The number of clusters obtained for each month is considered suitable whenever there is a minimum of overlapping cases from different clusters, and the members of each cluster share similar formation areas, velocities, and directions. We also carry out an analysis of variance (ANOVA) to decide whether the means of the position coordinates are significantly different between groups.

As mentioned in the previous section, the traditional seasons are not good discriminators of Mediterranean cyclone activity. Alpert et al. (1990b) pointed out that there are minor intermonthly cyclone route variations within each season, which actually seem to be slow transitions between the three most pronounced Mediterranean seasons: winter, spring, and summer. As before, we shall focus on January, April, and August.

The ANOVA results obtained for eight western Mediterranean clusters and five eastern clusters in January, nine western clusters and seven eastern clusters in April, and seven western clusters and six eastern clusters in August are statistically significant at $p < 1\%$. The F ratios and statistical significance should be regarded with caution, since the groups have already been arranged by the cluster algorithm to obtain the most significant ANOVA (Hartigan 1975). However, the mag-

nitude of the F values was such that not only are the average positions reasonably different between clusters, but also that both coordinates contributed significantly to the criteria for assigning tracks to each cluster. In general, the highest values of F occur for longitude coordinates, suggesting a stronger zonal classification, except for the eastern Mediterranean in April, where a more pronounced meridional stratification seems to emerge, and for the eastern Mediterranean in January, where zonal and meridional classifications seem to be equally important.

The cluster analysis performed over the 6-h cyclone positions revealed groups of trajectories with similar paths and also with similar velocities. January, April, and August results are shown in Figs. 10, 11, and 12, respectively, where average travelling cyclone routes and stationary or quasi-stationary cyclone positions are represented separately. The main trajectory bands and main areas of activity of each cluster are estimated by standard deviations of coordinates. A major feature present in the analysis consists of a clear increase of slow-moving or stationary cyclones toward August, as thermal processes tend to dominate over baroclinically driven lows.

The Bay of Biscay and central Iberia are the two main routes of January Atlantic depressions into the Mediterranean. Later in the year, the Biscay path tends to tilt to the northeast, decreasing its influence over the Med-

TABLE 5. Average and standard deviation of maximum deepening [$\text{hPa (6 h}^{-1})$] per cyclogenetic region. All values have been adjusted to 37.5°N reference latitude.

	January		April		August	
	Mean	Std dev	Mean	Std dev	Mean	Std dev
Sahara	—	—	3.56	2.508	2.45	2.029
Gulf of Genoa	1.89	2.088	1.37	1.391	1.03	1.139
Southern Italy	1.09	1.756	0.90	1.765	—	—
Cyprus	1.23	1.690	1.22	1.662	1.85	1.989
Middle East	1.72	1.731	1.55	1.605	2.04	1.674
Aegean Sea	1.43	1.708	1.52	1.241	—	—
Black Sea	1.32	1.671	1.46	1.637	0.61	0.906
Iberian peninsula	—	—	—	—	1.52	1.103
Whole area	1.52	1.949	1.69	1.903	1.41	1.419

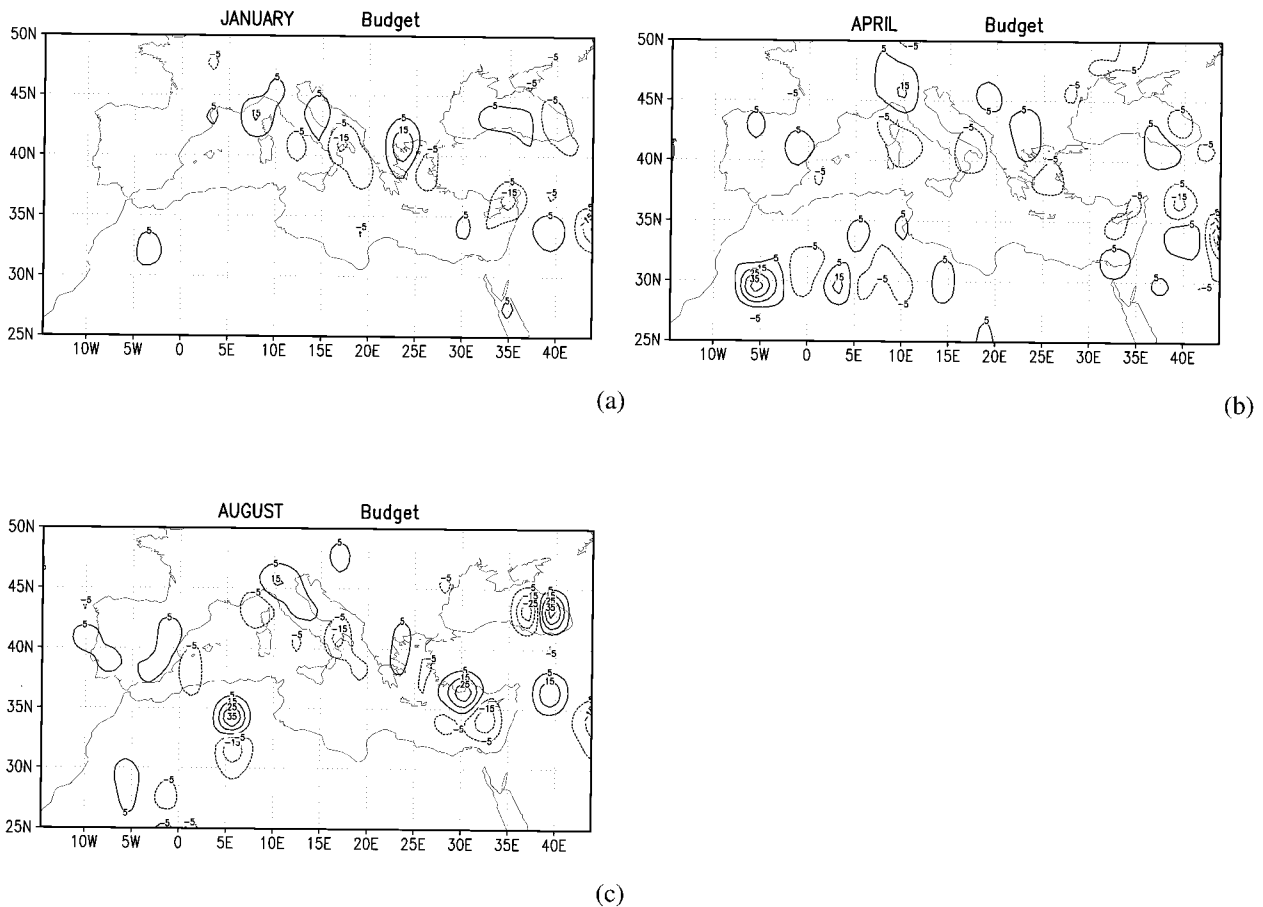


FIG. 9. Difference between the number of cyclones first detected and last detected within each $2.25^\circ \times 2.25^\circ$ cell. Positive (negative) contours indicate mainly cyclogenetic (cyclolysis) regions.

iterranean Sea, while central-southern Iberia becomes dominated by quasi-stationary lows.

The Gulf of Genoa region seems to have a more complex net of routes. In the winter there is a prevailing southeastward direction, extending through Italy, down to the Albanian and Greek coasts. During spring and summer a single slow-moving route and a quasi-stationary depression area, respectively, replace the winter

track, as a result of weaker baroclinicity over the northern Mediterranean coast.

An important northeastward path appears in April and August between the Balearic and Corsega Islands, explaining the cyclone sink area over the later region (Figs. 9b,c). Also in spring and summer there is a trajectory cluster associated with cyclones moving out of the Adriatic Sea into the Balkans.

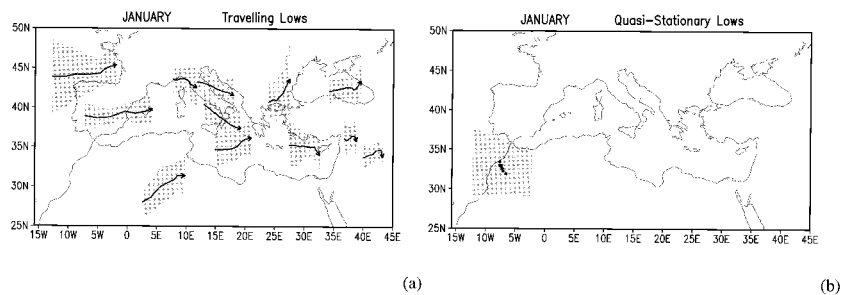


FIG. 10. Clusters' mean positions for Jan: (a) traveling cyclones, (b) quasi-stationary cyclones. The shaded regions represent the area of influence of each cluster, evaluated by the coordinates' standard deviation.

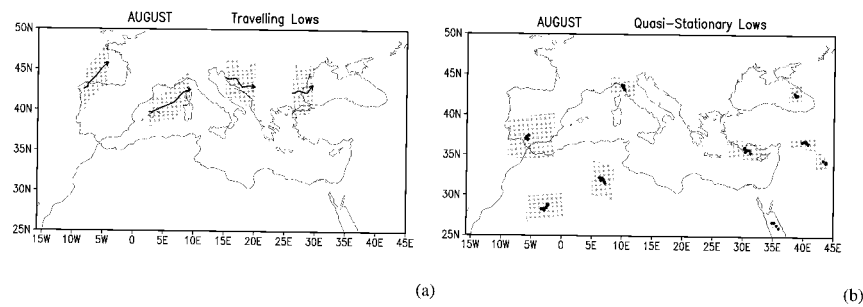


FIG. 11. As in Fig. 10, but for April.

As Atlantic troughs move over the African coast, baroclinic waves are formed south of the Atlas Mountains (Barry and Chorley 1992; Thorncroft and Flocas 1997), resulting in the quasi-stationary Saharan depression area observed in all months. A southward shift, and a decrease of the total area influenced by this particular cluster, toward summer is probably associated with the predominance of thermally driven processes. Also, there is a pronounced increase of cyclone routes over northern Africa in spring, when major eastward and northeastward paths appear roughly between 0° and 30°E . Most of the depressions moving northeastward are reinforced as they move into the Mediterranean Sea, causing large rainfalls over the Greek region (Flocas and Giles 1991).

Both western and eastern Black Sea coasts seem to be, almost permanently, two major cyclone paths. Sea-land contrast and associated low-level baroclinicity (Hoskins and Valdes 1990) may play an important role in their maintenance. In August, the eastern Black Sea path is substituted by a stationary low region as, in fact, are all main eastern Mediterranean routes—south of the Turkish coast, over Cyprus and Syria—as the Asian monsoon trough extends its influence to the Middle East and eastern Mediterranean Sea.

5. Conclusions

An objective methodology was employed to identify and track Mediterranean cyclones using the high-resolution ECMWF dataset, covering an 18-yr period. Cyclone characteristics were then evaluated and compared

with other Northern Hemisphere depressions, showing that in general Mediterranean lows are less intensive and are associated with smaller spatial scales and with shorter life cycles than Atlantic synoptic systems (on average 2–2.5 days less).

The most active Mediterranean regions were identified by computing cyclogenesis events for the whole area. It should be noticed that these include all the initial cyclone detections, that is, cyclones developing within the Mediterranean Basin plus cyclones entering the domain. The annual cyclogenesis distribution obtained seems to fit a three-season scheme well, where the conventional autumn months correspond to a rather sudden transition between summer and winter regimes.

In contrast with previous work, cyclogenesis maxima associated with subsynoptic-scale lows are clearly observed, namely, in the Aegean and Black Seas and over the Iberian peninsula during the summer. Strong cyclogenesis maxima were also found in the Gulf of Genoa region, south of the Atlas Mountains, and in the Middle East. While the latter might correspond to intrusions of the summer Asian monsoon into the Mediterranean basin, Genoa and Atlas lows seem to be mainly of lee cyclogenesis origin.

Cyclones developed in different regions within the Mediterranean area are shown to have quite different characteristics. In particular, it is worth noting the high frequency and the unexpectedly high intensity of spring lows over North Africa.

As pointed out by Barry and Chorley (1992), the movement of Mediterranean depressions is highly com-

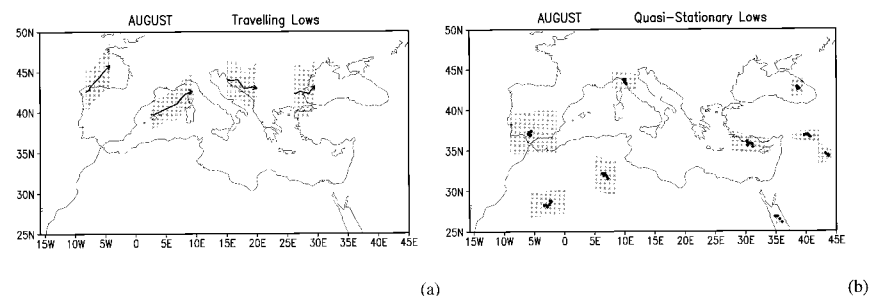


FIG. 12. As in Fig. 10, but for August.

plex due to both orographic effects and their regeneration over the sea. The k -means clustering technique proved to be useful in summarizing the analysis of more than 200 paths per month over the whole period. The clusters exhibit the main Mediterranean routes, some consistent with those found by HMSO (1962); for example, the incoming lows from the Atlantic through the Gulf of Biscay and southern Iberia in the winter, the spreading of North African tracks from the Atlas region in spring, the complex net of routes surrounding the Gulf of Genoa, and the cyclone track oriented to the eastern coast of the Mediterranean. The k -means method was also successful in grouping cyclone tracks with similar velocities. Clusters of stationary and quasi-stationary lows, increasing toward the summer, are clearly identified, especially over northern Africa, the Iberian Peninsula, the Middle East, Cyprus, and the Black Sea. However, the major steering mechanisms of Mediterranean lows, associated either with large-scale circulation regimes, or local effects, such as low-level baroclinicity induced by sea-land contrast, or local orography, are as yet unexplored. The relationship between the climatology of Mediterranean storm tracks presented in this paper and these, or any other mechanisms, will be the subject of a later paper.

Acknowledgments. The present work was supported by the PRAXIS XXI program (Portuguese Office for Science and Technology), Grant BD/9508/96. The ECMWF dataset was supplied by the British Atmospheric Data Centre. We are grateful for the helpful comments made by two anonymous reviewers.

REFERENCES

- Alpert, P., B. U. Neeman, and Y. Shay-El, 1990a: Climatological analysis of Mediterranean cyclones using ECMWF data. *Tellus*, **42A**, 65–77.
- , —, and —, 1990b: Intermonthly variability of cyclone tracks in the Mediterranean. *J. Climate*, **3**, 1474–1478.
- Barry, R. G., and R. J. Chorley, 1992: *Atmosphere, Weather and Climate*. 6th ed. Routledge, 392 pp.
- Blender, R., K. Fraedrich, and F. Lunkeit, 1997: Identification of cyclone track regimes in North Atlantic. *Quart. J. Roy. Meteor. Soc.*, **123**, 727–741.
- Buzzi, A., and S. Tibaldi, 1978: Cyclogenesis in the lee of Alps: A case study. *Quart. J. Roy. Meteor. Soc.*, **104**, 271–287.
- ECMWF, 1995: User guide to ECMWF products. Edition 2.1. Meteorological Bull. M3.2., 71 pp.
- Egger, J., P. Alpert, A. Tafferter, and B. Ziv, 1995: Numerical experiments on the genesis of Sharav cyclones: Idealised simulations. *Tellus*, **47A**, 162–174.
- Flocas, A. A., 1988: Frontal depressions over the Mediterranean sea and Central Southern Europe. *Mediterranée*, **4**, 43–52.
- , and B. D. Giles, 1991: Distribution and intensity of frontal rainfall over Greece. *Int. J. Climatol.*, **11**, 429–442.
- , and T. S. Karacostas, 1996: Cyclogenesis over the Aegean Sea: Identifications and synoptic categories. *Meteor. Appl.*, **3**, 53–61.
- Garrett, C., R. Outerbridge, and K. Thompson, 1993: Interannual variability in Mediterranean heat and buoyancy fluxes. *J. Climate*, **6**, 900–910.
- Hartigan, J. A., 1975: *Clustering Algorithms*. Wiley and Sons, 351 pp.
- HMSO, 1962: *Weather in the Mediterranean I: General Meteorology*. 2d ed. Her Majesty's Stationery Office, 362 pp.
- Hoskins, B. J., and P. J. Valdes, 1990: On the existence of storm-tracks. *J. Atmos. Sci.*, **47**, 1854–1864.
- Jacobbeit, J., 1987: Variations of trough position and precipitation patterns in the Mediterranean Area. *J. Climatol.*, **7**, 453–476.
- Lefevre, R. J., and J. W. Nielsen-Gammon, 1995: An objective climatology of mobile troughs in the northern hemisphere. *Tellus*, **47A**, 638–655.
- Mirkin, B., 1996: *Mathematical Classification and Clustering*. Kluwer Academic, 428 pp.
- Murray, R. J., and I. Simmonds, 1991: A numerical scheme for tracking cyclone centres from digital data. Part I: Development and operation scheme. *Aust. Meteor. Mag.*, **39**, 155–166.
- Nielsen, J. W., and R. M. Dole, 1992: A survey of extratropical cyclone characteristics during GALE. *Mon. Wea. Rev.*, **120**, 1156–1167.
- Peixoto, J. P., and A. H. Oort, 1992: *Physics of Climate*. American Institute of Physics, 520 pp.
- Petterssen, S., 1956: *Weather Analysis and Forecasting*. Vol. I, *Motion and Motion Systems*, McGraw-Hill, 428 pp.
- Radinovic, D., 1987: Mediterranean cyclones and their influence on the weather and climate. PSMP Rep Series 24, WMO, Geneva, Switzerland, 131 pp.
- Rodwell, M. J., and B. J. Hoskins, 1996: Monsoons and the dynamics of deserts. *Quart. J. Roy. Meteor. Soc.*, **122**, 1385–1404.
- Roebber, P. J., 1984: Statistical analysis and updated climatology of explosive cyclones. *Mon. Wea. Rev.*, **112**, 1577–1589.
- Serreze, M. C., 1995: Climatological aspects of cyclone development and decay in the Arctic. *Atmos.–Ocean*, **33**, 1–23.
- , F. Carse, R. G. Barry, and J. C. Rogers, 1997: Icelandic low cyclone activity: Climatological features, linkages with the NAO, and relationships with recent changes in the Northern Hemisphere circulation. *J. Climate*, **10**, 453–464.
- Sinclair, M. R., 1994: An objective cyclone climatology for Southern Hemisphere. *Mon. Wea. Rev.*, **122**, 1156–1167.
- Thorncroft, C. D., and H. A. Flocas, 1997: A case study of Saharan cyclogenesis. *Mon. Wea. Rev.*, **125**, 1147–1165.